Phase-shift modelling for HTI Media.

Ritesh K. Sharma[1] and Robert J. Ferguson[1]

1. Consortium for Research in Elastic Wave Exploration Seismology (CREWES), University of Calgary

Summary

Since fractures play an important role in hydrocarbon production as they determine the pathways and volume of crustal fluid movement. In behalf of the importance of the plane wave domain, we present phase shift modelling for HTI media in order to seek the effect of fractures on the travel time and amplitude of the body waves as these analysis can be useful for fractures analysis. We follow the almost same theory as discussed in paper entitled "*9C-3D* modeling for VTI media" only difference resides on the way of computing polarization angle. The investigation of the synthetic data for HTI media make it possible to conclude that P- and SH-waves amplitude are highest in the direction of fracture strike while SV-wave amplitude depends on the difference between ϵ and δ. The presented modelling will be contributive to fracture detention from the surface seismic data. Additionally, this modelling will be applicable for VSP and micro-seismicity modelling in the presence of anisotropy.

Kinematic and Dynamic analysis of seismic wave propagation in TI media.

- Using the equation of motion and Hooke's law, the wave equation can be represented as

$$\rho\frac{\partial^2 u_i}{\partial t^2} = c_{ijkl}\frac{\partial^2 u_k}{\partial x_l \partial x_j}. \quad (1)$$

- Substitution of the plane wave solution $u_k = AU_k e^{i\omega(n_j x_j/V - t)}$, into the wave equation leads to the Christoffel equation

$$\begin{bmatrix} G_{11}-\rho V^2 & G_{12} & G_{13} \\ G_{21} & G_{22}-\rho V^2 & G_{23} \\ G_{31} & G_{32} & G_{33}-\rho V^2 \end{bmatrix}\begin{bmatrix} U_1 \\ U_2 \\ U_3 \end{bmatrix} = 0, \quad (2)$$

with G_{ik}=$c_{ijkl} n_j n_l$ and **U** is the polarization vector, ω is the angular frequency, **n** is the unit wavefront normal and V is the phase velocity.

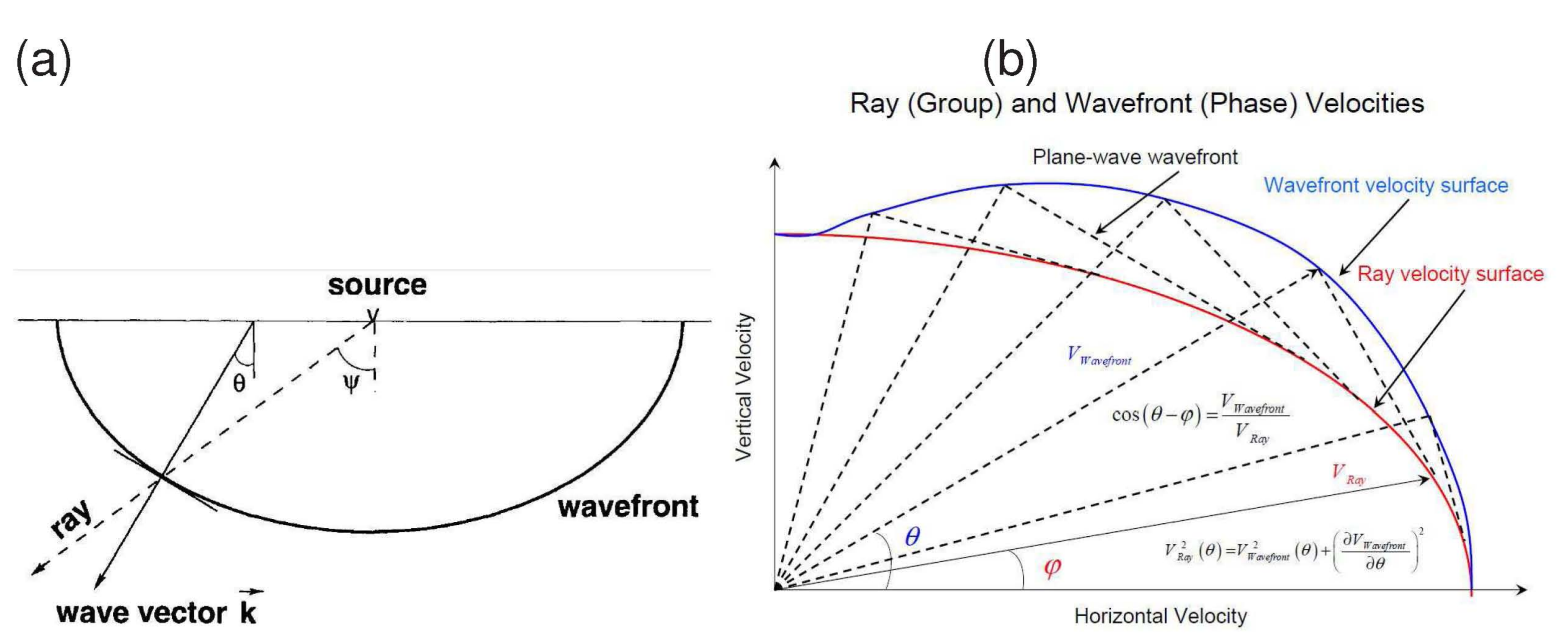

Fig.1: Schematic representation of group and phase (a) angles and (b) velocity surfaces.

Implementation of the proposed modelling

- Extrapolation of the source spectrum φ_0 to a new depth Δz as

$$\varphi_{\Delta z} = \varphi_0 e^{i\,\Delta z\, q\,\omega}. \quad (3)$$

- Build a rotation matrix based on the polarization angle (θ_1) of P wave-

Implementation of our method

source and azimuth (ϕ).

$$R(\theta_1,\phi) = \begin{bmatrix} \cos\phi & \sin\phi\cos\theta_1 & \sin\theta_1\sin\phi \\ -\sin\phi & \cos\phi\cos\theta_1 & \cos\phi\sin\theta_1 \\ 0 & -\sin\theta_1 & \cos\theta_1 \end{bmatrix}. \quad (4)$$

- In order to obtain the polarization angle (θ_1) first the propagation angle (θ) is computed as

$$\sin\theta = \left|\hat{\mathbf{p}}\times\hat{\mathbf{a}}\right|, \quad (5)$$

$\hat{\mathbf{p}}$ and $\hat{\mathbf{a}}$ are known the unit normals. Once the propagation angle is known, the polarization angle is computed as

$$\theta_1 = \tan^{-1}\frac{\left(\alpha^2(\theta) - \beta_0^2\sin^2\theta - \alpha_0^2\cos^2\theta\right)}{\sqrt{\left[\alpha_0^2-\beta_0^2\right]\ \left[\alpha_0^2\left[2\,\delta+1\right]-\beta_0^2\right]}\ \sin\theta\,\cos\theta}. \quad (6)$$

- Apply the rotation matrix to the extrapolated wavefield as

$$D = R(\theta_1,\phi)\,W, \quad (7)$$

where D=$[H_1,\ H_2,\ V]'$ is the source wavefield rotated into the orientation of the 3C geophone. where H_1, H_2, and V are the cross-line, in-line and vertical components of the vector wavefield respectively.

- Extract the desired component for analysis.

Examples

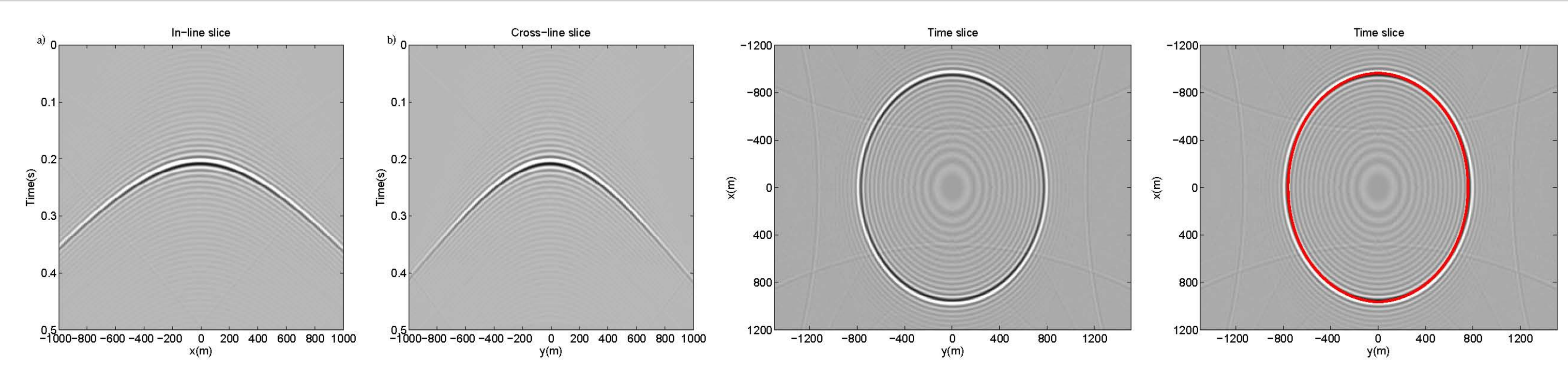

Fig.2: In-line, Cross-line and time slices of the P wave extrapolated wavefield for HTI media. The effect of fractures, kinematically & dynamically, is demonstrated in this figure as well as in following figures. The authentication of the proposed modelling is demonstrated here as analytic curve (shown in red) is ana- -logous to obtained one. More energy is concerned in the direction of fracture strike.

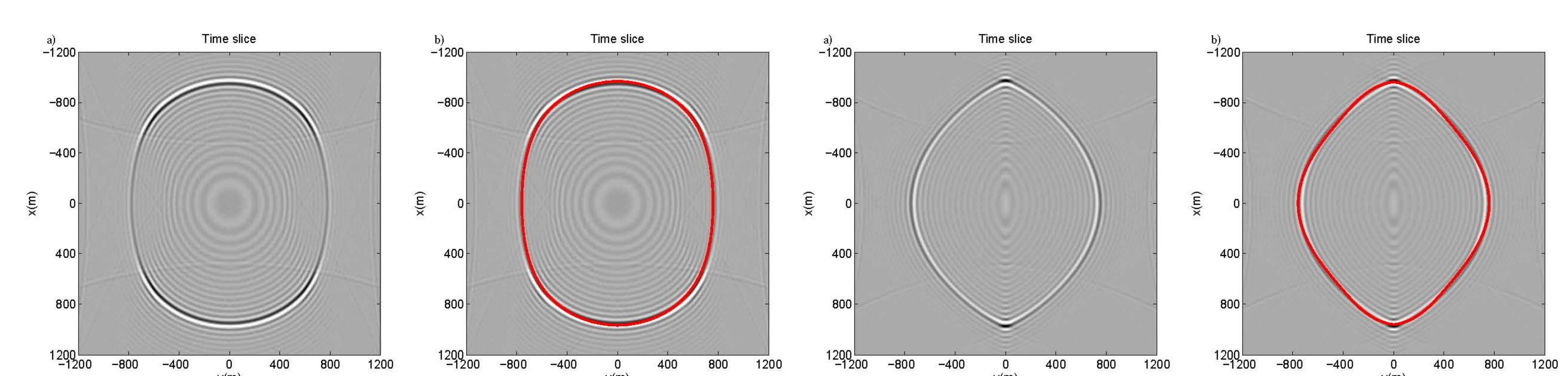

Fig.3: Time slices of the extrapolated P wavefield in HTI media after introducing higher anisotropy reveal the influence of the magnitude of the anisotropy on kinematic and dynamic analysis. .

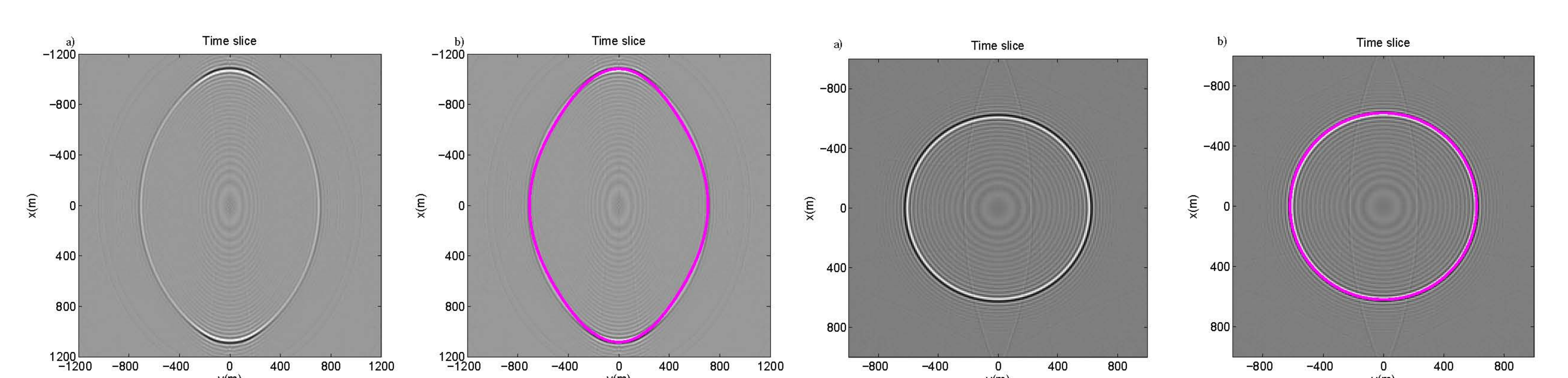

Fig.4: Time slices of the extrapolated SH wavefield and SV wavefield for a medium where $\epsilon > \delta$.

Examples

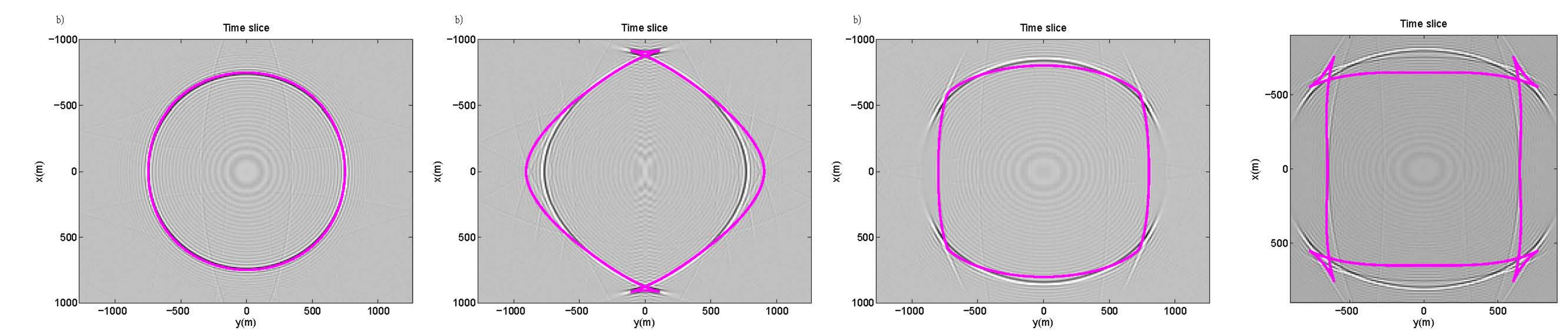

Fig.5: Time slices of the extrapolated SV wavefield for different different mediums possess $\epsilon > \delta$, negative δ and more negative δ. The triplication behaviour of SV-wave is revealed.

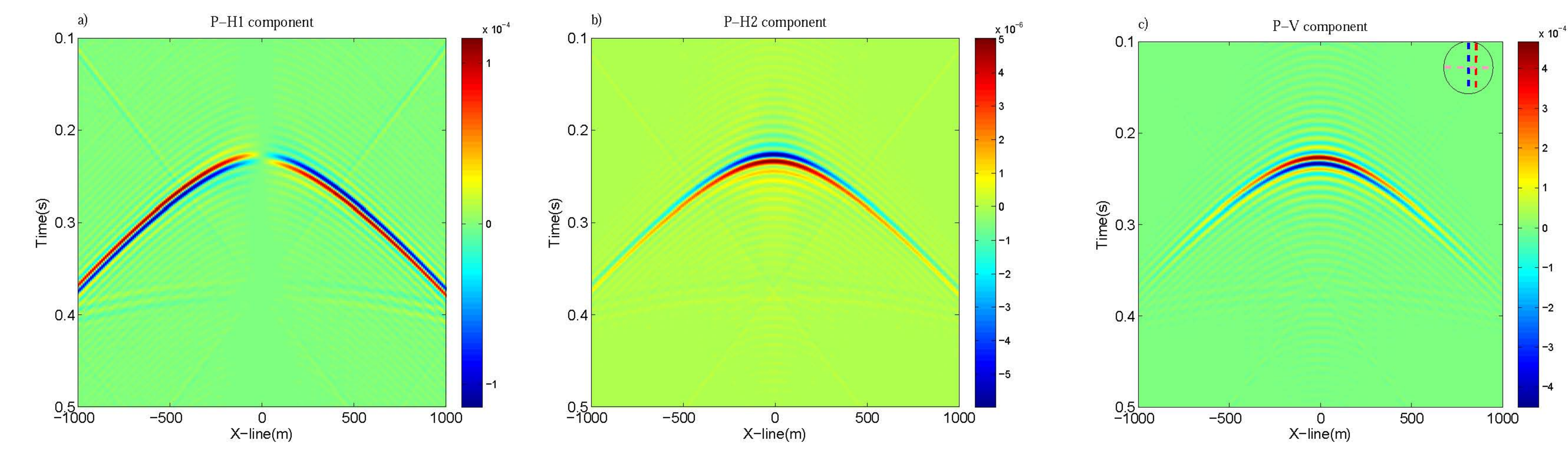

Fig.6: Registered energy versus offset (REVO) analysis of P wave source illustrate the favourable condition of energy registration on different components of 3C geophone.

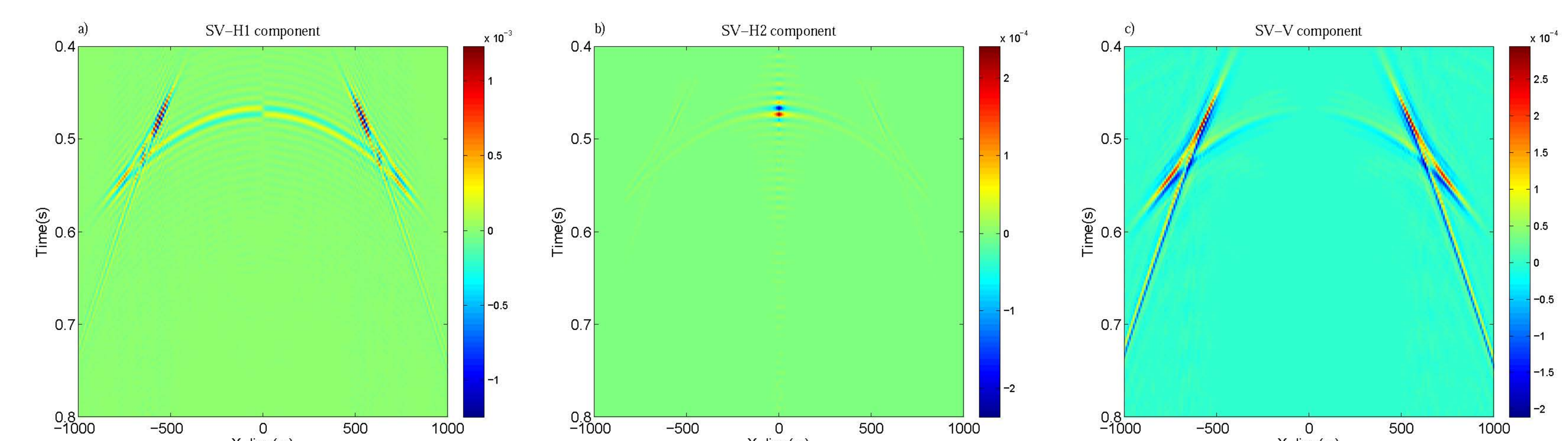

Fig.7: REVO analysis of SV wave source on different components illustrate that the energy registration decreases with offset on H_1 and H_2 while increases on vertical component. The triplication phenomena is noticed.

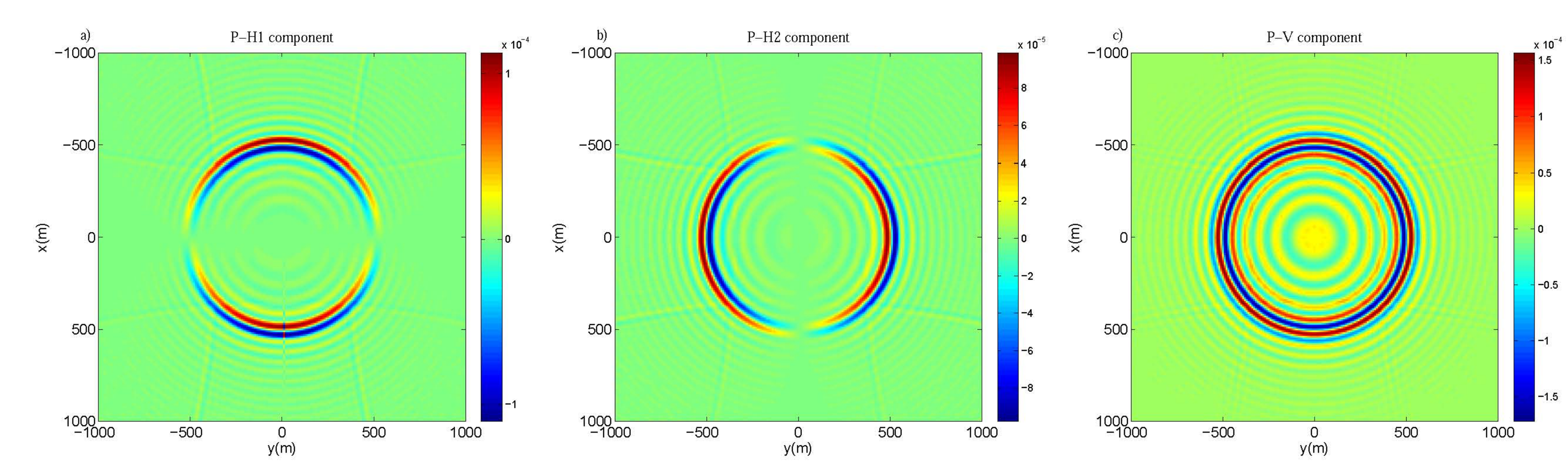

Fig.8: Registered energy versus azimuth (REVA) analysis of P wave source on different components for VTI media.

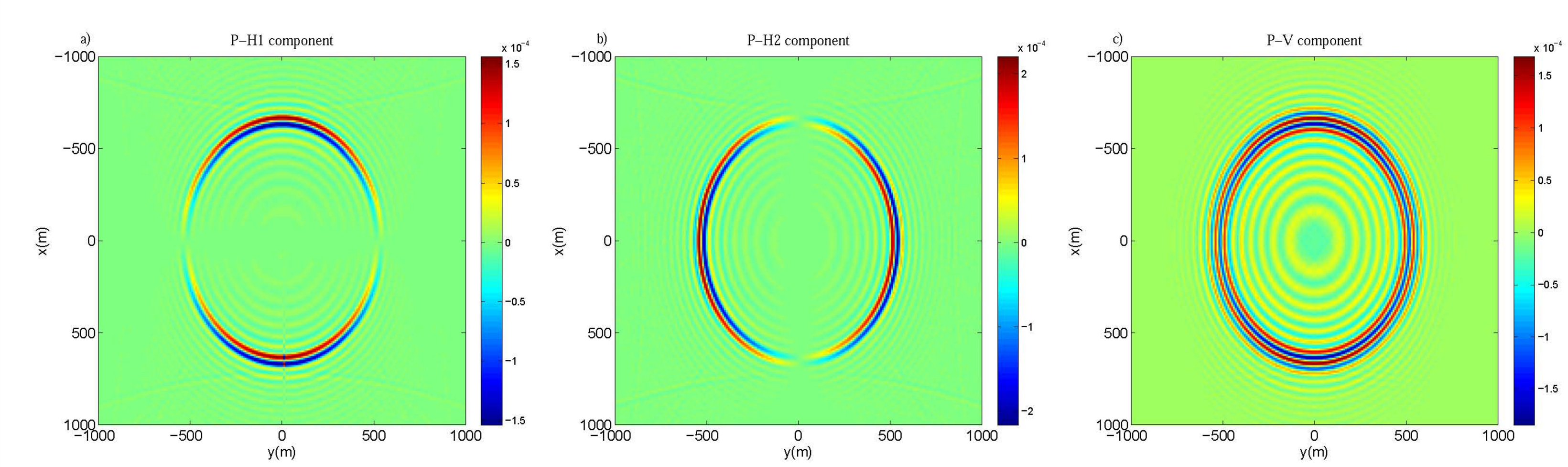

Fig.9: REVA analysis of P wave source on different components for HTI media.

Acknowledgments

- We thank the sponsors of CREWES for financial supports. We thank students and support staff of CREWES.